

# Electron emission characteristics of GaN pyramid arrays grown via organometallic vapor phase epitaxy

Cite as: Journal of Applied Physics **84**, 5238 (1998); <https://doi.org/10.1063/1.368775>  
Submitted: 27 March 1998 • Accepted: 06 August 1998 • Published Online: 14 October 1998

B. L. Ward, O.-H. Nam, J. D. Hartman, et al.



View Online



Export Citation

## ARTICLES YOU MAY BE INTERESTED IN

[GaN nanotip pyramids formed by anisotropic etching](#)

Journal of Applied Physics **94**, 650 (2003); <https://doi.org/10.1063/1.1582233>

[Strain-induced polarization in wurtzite III-nitride semipolar layers](#)

Journal of Applied Physics **100**, 023522 (2006); <https://doi.org/10.1063/1.2218385>

[Magnesium induced changes in the selective growth of GaN by metalorganic vapor phase epitaxy](#)

Applied Physics Letters **72**, 921 (1998); <https://doi.org/10.1063/1.120874>



Applied Physics  
Reviews

Read. Cite. Publish. Repeat.

**19.162**  
2020 IMPACT FACTOR\*



# Electron emission characteristics of GaN pyramid arrays grown via organometallic vapor phase epitaxy

B. L. Ward, O.-H. Nam, J. D. Hartman, S. L. English, B. L. McCarron, R. Schlessler, Z. Sitar, R. F. Davis, and R. J. Nemanich<sup>a)</sup>

*Department of Physics and Department of Materials Science and Engineering, North Carolina State University, Raleigh, North Carolina 27695-8202*

(Received 27 March 1998; accepted for publication 6 August 1998)

Selective growth of arrays of silicon-doped GaN (Si:GaN) pyramids for field emitter applications has been achieved. The electron emission characteristics of these arrays has been measured using techniques such as field emission, field emission energy distribution analysis (FEED), photoemission electron microscopy (PEEM), and field emission electron microscopy (FEEM). The field emission current–voltage ( $I$ – $V$ ) results indicate an average threshold field as low as  $7\text{ V}/\mu\text{m}$  for an emission current of 10 nA. It is suggested that the low threshold field value is a consequence of both the low work function of Si:GaN and the field enhancement of the pyramids. The results of the FEEM and FEED measurements indicate agreement with the field emission  $I$ – $V$  characteristics. The FEED results indicate that the Si:GaN pyramids are conducting, and that no significant ohmic losses are present between the top contact to the array and the field emitting pyramids. The PEEM and FEEM images show that the emission from the arrays is uniform over a  $150\text{ }\mu\text{m}$  field of view.  
© 1998 American Institute of Physics. [S0021-8979(98)05321-3]

## I. INTRODUCTION

The growth of GaN by organometallic vapor phase epitaxy (OMVPE) has received much attention recently for both photonic and electronic device applications. The relatively strong atomic bonding of GaN points to its potential use in high-power and high-temperature microelectronic devices. Silicon doping of GaN has been shown to yield  $n$ -type material with a net carrier concentration as high as  $1E + 20\text{ cm}^{-3}$ .<sup>1</sup> The wurtzitic phase of GaN forms continuous solid solutions with InN and AlN such that band gap engineering is possible from 1.95 to 6.2 eV which leads to a range of photonic applications. Moreover, the electron affinity of GaN has been measured to be 3.3 eV by ultraviolet photoemission spectroscopy (UPS).<sup>2</sup> For an  $n$ -type material, this will be the work function which is substantially lower than most metals. In addition, GaN is not sensitive to atmospheric exposure with oxidation limited to less than 5 at. %.

Studies of the selective growth of intrinsic GaN pyramids have previously been reported.<sup>3–5</sup> One advantage of the selective growth process is the ability to form three-dimensional microstructures without the need for etching. Recently, field emission results have been reported from intrinsic GaN pyramid arrays.<sup>4–7</sup> In one study,<sup>4</sup> the  $I$ – $V$  characteristics indicated a current of  $0.8\text{ }\mu\text{A}$  at 2000 V applied over a distance of approximately 0.5 mm. In another study,<sup>5</sup> the current–voltage ( $I$ – $V$ ) characteristics indicated a current of  $80\text{ }\mu\text{A}$  at 1100 V applied over a distance of approximately 0.5 mm. Previously,<sup>6,7</sup> we reported some initial field emission findings from a silicon-doped GaN (Si:GaN) pyramid array. At an anode-to-sample spacing of  $27\text{ }\mu\text{m}$ , an emission current of 10.8 nA at 680 V was measured. These results are

promising and warrant a further investigation into the electron emission properties of GaN pyramid arrays.

There are three challenges concerning the application of field emission to microelectronics that will be addressed in this study: (1) The electron transport to the surface of the field emitting layer, (2) the uniformity and the control of the emission over a broad area of the sample, and (3) obtaining a threshold field suitable for field emission applications. The silicon doping of GaN will provide conduction band electrons which should be available for field emission into vacuum. Uniformity of electron emission has always been a challenge with flat films,<sup>8,9</sup> but an array of field emitting pyramids may offer a more uniform distribution of emission sites and better control of the electron emission. Last, the low work function of GaN will allow emission at low fields. This study focuses on the electron emission characteristics of an array of Si:GaN pyramids which could prove to be of significant importance for the development of vacuum microelectronic devices.

## II. EXPERIMENTS AND DATA ANALYSIS

Silicon-doped ( $\text{Si}:2E + 18\text{ cm}^{-3}$ ) GaN films  $1$ – $2\text{ }\mu\text{m}$  thick were grown on the (0001) face of  $n$ -type 6H–SiC with a  $0.1\text{ }\mu\text{m}$  AlN buffer layer. The growth conditions for these films is described elsewhere.<sup>1,10</sup> The masking step involved a  $\text{SiO}_2$  ( $0.1\text{ }\mu\text{m}$  thick) pattern with  $5\text{-}\mu\text{m}$ -diam holes spaced  $15\text{ }\mu\text{m}$  apart. The patterning was achieved using standard photolithographic techniques. The patterned area is typically  $0.5 \times 0.5\text{ mm}^2$  so that the number of pyramids in the array is about 1200. Prior to selective growth, the samples were cleaned in a buffered HCl solution to remove any surface oxide on the undergrown GaN layer. The selective growth was conducted at a temperature of  $1000$ – $1050\text{ }^\circ\text{C}$  at a pres-

<sup>a)</sup>Electronic mail: robert\_nemanich@ncsu.edu

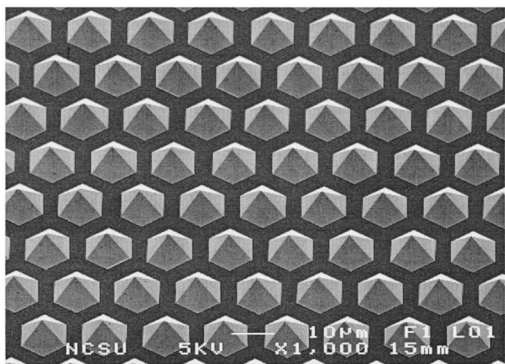


FIG. 1. SEM image of a Si:GaN pyramid array prepared by selective growth using OMVPE.

sure of 45 Torr. The triethylgallium flow rate was 26.1–70.0  $\mu\text{mol}/\text{min}$ . Silicon doping was carried out with  $\text{SiH}_4$  at 5.5 nmol/min during the selective growth process although the actual doping profile in the pyramids is unknown. After the selective growth process, the  $\text{SiO}_2$  is removed with a buffered HF solution. The pyramids truncate into a point having a tip radius  $\leq 100$  nm and an apex angle of  $56^\circ$  between the (1–101) facets. A more detailed description of the selective growth process is given elsewhere.<sup>6,7</sup> A scanning electron micrograph (SEM) of the resulting pyramid array is shown in Fig. 1.

Electrical measurements of top and back contacts to Si:GaN films grown on 6H–SiC with an AlN buffer layer have indicated that no current will traverse the AlN buffer layer. This highly resistive AlN buffer layer prevents electron injection directly from the SiC substrate into the Si:GaN, therefore a top contact must be made to the GaN. An ohmic contact of Ti(200 Å)/Au(1500 Å) is electron beam evaporated onto one corner of the sample. This Ti/Au pad will provide both the top contact during the field emission measurements as well as the Fermi level calibration in the field emission energy distribution (FEED) analysis.

The field emission measurements were conducted in a multiple chamber system interconnected with an ultrahigh vacuum (UHV) sample transfer mechanism. The system includes surface characterization, surface preparation and cleaning, and film growth capabilities. For this study, Auger electron spectroscopy (AES) was employed to monitor the surface contaminants, a remote plasma system was employed for surface cleaning and the field emission measurements were also obtained.

The wafers were exposed to ambient air for several days prior to the field emission measurements. After loading the sample into the UHV system, AES detected the presence of oxygen and carbon on the surface of the GaN. The amount of oxygen on the surface of the GaN was no more than 5 at. %. After initial field emission measurements a remote hydrogen plasma was employed for *in situ* surface cleaning. The remote hydrogen plasma was generated with radio frequency excitation at a power of 20 W. The flow rate of  $\text{H}_2$  was 82 sccm. The hydrogen plasma exposure was for 300 s while the sample was held at room temperature. The remote hydrogen plasma has demonstrated effective removal of surface

carbon contaminants, and in this case the surface carbon was reduced to near the detection limit of the AES. The process did not appear to have any affect on the Ga/N ratio or the surface oxygen as indicated by AES.

The field emission measurements employed a moving anode which was stepped toward the surface with  $I$ – $V$  measurements obtained at various anode-to-sample distances. The measurements were conducted with pressures typically  $< 1.0E-08$  Torr. The anode selected for these experiments was a molybdenum rod (3 mm diam). The end of the rod was either polished flat or polished to a very high radius of curvature, typically  $\geq 5$  mm. The anode is mounted on a stage which is coupled to a UHV stepper motor. The stepper motor controls the distance between the anode and the sample such that one step of the stepper motor yields a translation of 0.055  $\mu\text{m}$ .  $I$ – $V$  measurements were obtained with a computer controlled Keithley 237 Source Measure Unit (SMU). The SMU has the ability to simultaneously source a voltage and measure a current. A current limiting circuit is also included within the SMU. The maximum current, termed the compliance value, is controlled so that no voltage is applied which causes the current to exceed the compliance value. In our experiments the compliance current was  $1.0E-07$  A. In previous work on field emission from flat films, we have found that samples that emit at high threshold fields ( $> 30$  V/ $\mu\text{m}$ ) cannot yield large currents without damage. We have also found that samples that emit at low threshold fields ( $\leq 30$  V/ $\mu\text{m}$ ) can indeed yield large currents without damage. It is for this reason that we have limited the current to  $1.0E-07$  A in all of our field emission measurements.

For any given field emission measurement, a family of  $I$ – $V$  curves is obtained with each curve corresponding to a different anode-to-sample spacing. Initially, the anode is positioned at some unknown distance above the sample surface. The count value on the stepper motor controller is recorded and an  $I$ – $V$  curve is initiated. Once the  $I$ – $V$  curve is collected by the computer, the anode is moved closer to the sample by a fixed number of steps, and the cycle is repeated. After a sufficient number of  $I$ – $V$  curves is collected, the last count value is recorded and the experiment is terminated. The relative distances of all of the previously collected  $I$ – $V$  curves can be calculated with the knowledge of the step size. This technique has the advantage that the sample is never in contact with the anode.

The FEED measurements were performed in a separate chamber under UHV conditions using a VG CLAM II electron spectrometer. Details on the characterization of wide band gap materials using the FEED technique have been published recently.<sup>11</sup> The GaN sample was mounted on a negatively biased sample holder (up to  $-1100$  V) so that it faced the spectrometer entrance. The bias voltage was applied to the Ti/Au contact on the top of the GaN film. A sharpened tungsten tip (apex radius: 10  $\mu\text{m}$ ) was used as an extraction electrode. The sample was maneuvered to approximately 50  $\mu\text{m}$  from the extraction electrode on three different regions of the sample in order to extract electrons from (1) the Ti/Au contact, (2) a flat region on the GaN sample, and (3) the GaN pyramid array. Both the extraction electrode and the spectrometer were kept at ground potential.

It has been reported previously that electron emission from flat films yields the formation of “hot spots” of current that turn on and then turn off apparently at random with the application of a high electric field.<sup>8</sup> Photoemission electron microscopy (PEEM) and field emission electron microscopy (FEEM) are two techniques that can be employed to display the electron emission from surfaces.<sup>8,9</sup> This technique has the advantage over other techniques in that the emitted electrons are actually imaged so the source of emission can be readily identified. In this study, PEEM and FEEM are employed to examine the emission from the Si:GaN pyramid array. In the PEEM measurements, photoelectrons are excited by ultraviolet radiation from a 100 W Hg arc lamp. These photoelectrons are accelerated into an immersion objective lens. In this lens, 20 kV is applied over a distance of 2 mm resulting in an average field of 10 V/ $\mu\text{m}$ . Once the photoemitted electrons accelerate through the objective, they are magnified and focused by a series of lenses onto a microchannel plate and phosphor screen. A charge coupled device (CCD) camera records the image. Without the ultraviolet illumination, the microscope works as a FEEM. In FEEM, the only electrons that contribute to the image are those that are excited by the negative high bias applied to the sample mount ( $\sim 10$  V/ $\mu\text{m}$ ). The PEEM and FEEM measurement techniques and applications have been discussed in more detail elsewhere.<sup>12–17</sup>

### III. RESULTS AND DISCUSSION

After loading the Si:GaN pyramid sample into UHV and directly into the field emission chamber, the measurements were relatively unstable (noisy) and a high field emission threshold was obtained. The sample was then transferred to the remote plasma system and processed with a hydrogen plasma to remove surface contaminants.

After the H-plasma processing a significant reduction in the field emission threshold was obtained, and the measurements were repeatable and did not display the noise of the measurements of the as-loaded sample. A total of 34  $I$ - $V$  curves were obtained at different anode-to-surface distances. In order to verify Fowler–Nordheim tunneling, all of the  $I$ - $V$  curves were fit to the general form of the Fowler–Nordheim equation

$$I = aV^2 \exp(-b/V),$$

where  $I$  is the measured current,  $V$  is the applied anode voltage and  $a$  and  $b$  are used as fitting parameters. Examples of the measured  $I$ - $V$  curves are shown in Fig. 2(a). Each  $I$ - $V$  curve corresponds to a different anode to sample spacing. The  $I$ - $V$  data were fit to the Fowler–Nordheim equation. The Fowler–Nordheim expression was able to accurately fit all of the data suggesting that the emission process is tunneling. The  $a$  values ranged over many orders of magnitude and exhibited no direct correlation to the relative distance. The  $b$  values ranged from  $4E+04$  to  $4E+03$  V and also exhibited no direct correlation to the relative distance. With the exponential character of the Fowler–Nordheim  $I$ - $V$  equation, there is no well defined emission threshold. However, for comparison it is helpful to establish a threshold emission current. In this study 10 nA was used as the threshold current

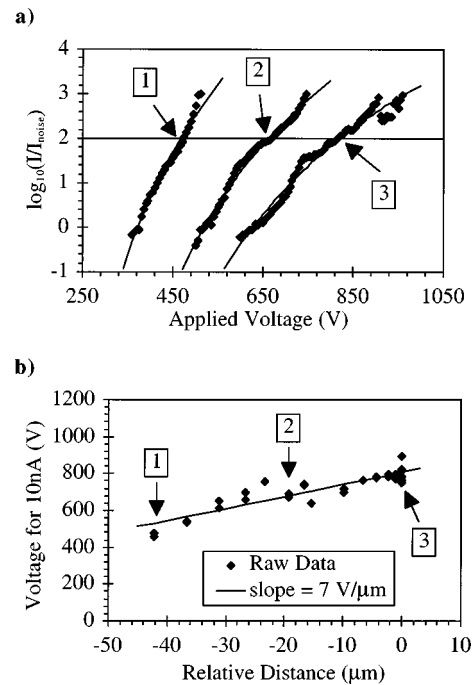


FIG. 2. (a) Field emission  $I$ - $V$  characteristics of the Si:GaN pyramid array shown in Fig. 1 after remote hydrogen plasma exposure. A total of 34  $I$ - $V$  curves were obtained in this experiment. 3 of the 34  $I$ - $V$  curves are shown. The  $I$ - $V$  data (dots) were fit to the Fowler–Nordheim equation (lines).  $I_{\text{noise}}$  is 0.1 nA. (b) The voltage for 10 nA of current is plotted vs the relative distance from the first  $I$ - $V$  measurement (step size =  $0.055 \mu\text{m}$ ). The slope of the line determines the average threshold field for 10 nA.

and the voltage that results in a current of 10 nA was then used as the threshold voltage for electron emission. This value of current was selected because it is two orders of magnitude above the inherent noise which was measured to be about  $1.0E-10$  A, and one order of magnitude below the compliance value, defined previously as  $1.0E-07$  A. The average threshold field (for 10 nA current) can be calculated for a single  $I$ - $V$  curve as the threshold voltage divided by the absolute anode-to-sample distance if a parallel plate geometry is assumed. This average threshold field is a macroscopic field value and should not be confused with the microscopic local field value at the cathode surface. Since at no point in the measurement process is the absolute distance known, an alternative method for obtaining the average threshold field was employed.

Each threshold voltage was plotted versus relative distance, and as expected, the resulting graph was linear as shown in Fig. 2(b). The relative distance scale in Fig. 2(b) is calculated using the first  $I$ - $V$  measurement as the “zero” distance point. The relative distances of all of the subsequently measured  $I$ - $V$  curves can be calculated with the knowledge of the step size. Upon fitting the data to a straight line, an average threshold field for 10 nA can be obtained from the slope of the line as indicated in Fig. 2(b). This technique for determining the average threshold field for 10 nA does not rely upon the absolute anode-to-sample distance but rather the change in distance of the anode with respect to the sample, or the step size. The average threshold field for

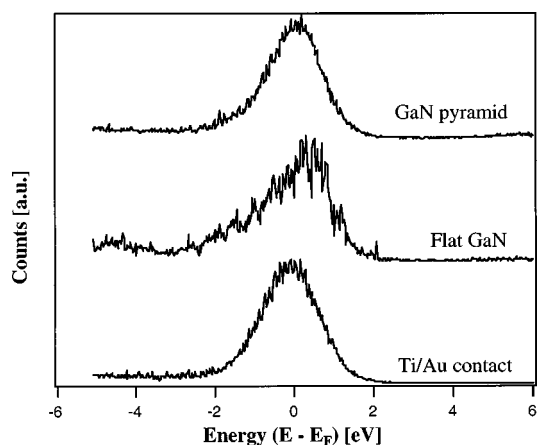


FIG. 3. FEED spectra recorded from three different regions of the sample. The peak of the energy distribution did not shift indicating all regions were at the same potential.

10 nA obtained from the pyramid array in this experiment was  $7 \text{ V}/\mu\text{m}$ .

The technique employed here effectively measures the average field in the vacuum region above the sample. Two aspects that may confuse the situation are field enhancement at the surface due to the morphology, and field penetration into the emitting sample. Certainly we are relying on the morphology of the tips to lead to field enhancement, so this effect is expected here. The question of field penetration can be addressed with the FEED measurements.

Two important techniques for understanding electron emission mechanisms are the FEED measurement and UPS. FEED analysis consists of measuring the energy spectrum of field-emitted electrons by means of an electron spectrometer. The FEED and UPS techniques are similar in that the energy of the emitted electrons is analyzed. However, their respective methods of excitation yields significant differences in the resulting energy spectrum. With FEED, any local field enhancement such as protrusions or surface roughness will dominate the electron emission so that the resulting analysis may not be a global average of the emission properties of the surface. With UPS, however, the light will excite electrons from a large portion of the sample that is only limited in size to the spot diameter of the excitation source. The two techniques reveal different information about the electron emission characteristics of the sample. In UPS, a positive electron affinity can be quantified and a negative electron affinity can be determined from the width of the spectrum along with the knowledge of the band gap of the material and the energy of the excitation source. In FEED, information about how the electrons are transported through the material and from where the electrons originate can be obtained from the peak position, the full width at half maximum, and the general shape of the FEED spectrum.

FEED spectra were recorded in all three regions and are displayed in Fig. 3 on a normalized energy scale. The origin of the energy scale in Fig. 3 coincides with the kinetic energy of electrons emitted from the Fermi level of the metallic contact. To obtain adequate counting rates, all spectra were obtained at a relatively low resolution of  $0.5 \pm 0.1 \text{ eV}$ . It is

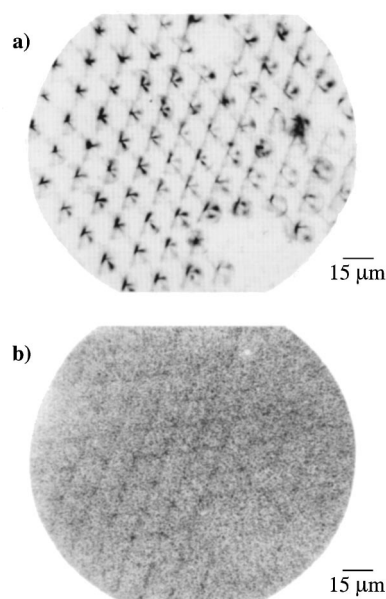


FIG. 4. (a) PEEM image and (b) FEEM image with the focal plane at the tips of the Si:GaN pyramid array. The field of view is  $150 \mu\text{m}$ . The dark regions represent areas of electron emission.

apparent that the peak of the energy distribution of electrons emitted from the three regions was virtually identical as can be seen in Fig. 3. In particular, none of the peaks showed a voltage-dependent shift (on the energy scale relative to the Fermi level,  $E - E_F$ ) as the bias voltage was changed in a range from  $-400$  to  $-1100 \text{ V}$ . This observation demonstrates that the electrons originate from near the Fermi level of the sample. Therefore, no significant potential drop occurred between the contact area and the emission sites. Hence, in contrast to the earlier measurements of diamond and *c*-BN,<sup>11</sup> the *n*-type doped GaN exhibited a metallic-like conductivity in the base GaN film as well as in the pyramids which significantly enhanced electron transport through the bulk.

PEEM and FEEM images are shown in Figs. 4–7. Figures 4(a) and 4(b), respectively, show  $150 \mu\text{m}$  field of view

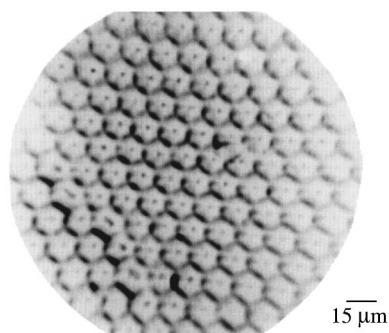


FIG. 5. PEEM image with the focal plane at the base of the Si:GaN pyramid array. The field of view is  $150 \mu\text{m}$ . The corresponding FEEM image was faint but discernible indicating that emission occurs from any of the sharp features in the pyramid array. The dark regions represent areas of electron emission.

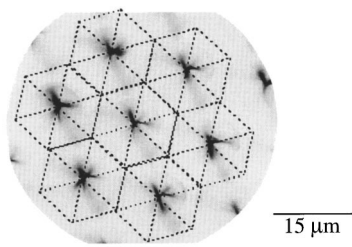


FIG. 6. High magnification PEEM image of the Si:GaN pyramid array. The field of view is  $50\ \mu\text{m}$  and the focal plane of the microscope intersects the top of the pyramid array. The dark regions represent areas of electron emission.

PEEM and FEEM images on the same area of the pyramid array. Because of the limitations of the depth of view of the microscope, it is important to note that the tips of the pyramids are being imaged because the focal plane of the microscope intersects the top of the pyramid array. If we were to adjust the focal plane to intersect the base of the pyramid array, then the image shown in Fig. 5 is obtained. The corresponding FEEM image to Fig. 5 was faint but discernible. Figures 6 and 7 are PEEM images with a  $50\ \mu\text{m}$  field of view. In Fig. 6, the focal plane of the microscope intersects the top of the pyramid array and in Fig. 7, the focal plane intersects the base of the pyramid array. At this time, we do not understand the origin of the emission in Figs. 5 and 7. No FEEM images for a field of view less than  $150\ \mu\text{m}$  could be discerned in this experiment.

For all of the tips in the  $150\ \mu\text{m}$  field of view, the electron emission seemed to be uniform as indicated in Fig. 4(b). The uniformity of the pyramid array offers several advantages over flat films. With flat films, the formation of random hot spots of current is not a useful property for microelectronic applications. It is very important to be able to control the amount of current from the sample, the stability of that current and from where that current originates. The use of the pyramids as a source of electrons allows the current stability and uniformity requirements of microelectronic applications to be a realizable possibility.

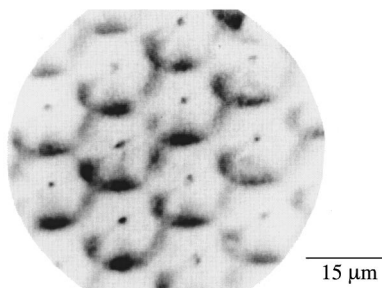


FIG. 7. High magnification PEEM image of the Si:GaN pyramid array. The field of view is  $50\ \mu\text{m}$ , and the focal plane of the microscope intersects the base of the pyramid array. The dark regions represent areas of electron emission.

#### IV. CONCLUSIONS

We have characterized the electron emission of Si:GaN pyramid arrays. Uniform pyramid arrays of GaN with silicon doping can be fabricated without the use of etching. The growth of the pyramid arrays can be accomplished by a selective epitaxial process. Three characterization techniques were used to study the electron emission from the field emitting array including field emission  $I$ - $V$  measurements, FEED analysis, PEEM, and FEEM. To obtain stable emission at low applied fields it was necessary to expose the surface to a hydrogen plasma cleaning process. After surface preparation field emission  $I$ - $V$  measurements indicated an average threshold field value as low as  $7\ \text{V}/\mu\text{m}$ . The FEED measurement indicated emission from the Fermi level of the Si:GaN indicating no field penetration. PEEM and FEEM indicated uniformity of the electron emission over a  $150\ \mu\text{m}$  field of view. The FEEM measurement indicated agreement with the field emission  $I$ - $V$  measurement. The low work function and geometric field enhancement of the Si:GaN pyramid array as well as the availability of electrons in the bulk of the material contribute to the uniform electron emission at low macroscopic threshold fields. While the goal of this work was to study the electron emission mechanisms involved, more work needs to be done to establish whether the Si:GaN pyramid arrays will be a competitive technology with current field emitter arrays. Future work should include measurements at higher fields to extract higher emission currents to test the current yield as well as the mechanical stability of the pyramid array.

#### ACKNOWLEDGMENT

This study was supported by the Office of Naval Research.

- <sup>1</sup>T. W. Weeks, Jr., M. D. Bremser, K. S. Ailey, E. Carlson, W. G. Perry, and R. F. Davis, *Appl. Phys. Lett.* **67**, 401 (1995).
- <sup>2</sup>M. C. Benjamin, M. D. Bremser, T. W. Weeks, Jr., S. W. King, R. F. Davis, and R. J. Nemanich, *Appl. Surf. Sci.* **104/105**, 455 (1996).
- <sup>3</sup>S. Kitamura, K. Hiramatsu, and N. Sawaki, *Jpn. J. Appl. Phys., Part 2* **34**, L1184 (1995).
- <sup>4</sup>R. D. Underwood, D. Kapolnek, B. P. Keller, S. Keller, S. P. DenBaars, and U. K. Mishra, *Solid-State Electron.* **41**, 243 (1997).
- <sup>5</sup>D. Kapolnek, R. D. Underwood, B. P. Keller, S. Keller, S. P. DenBaars, and U. K. Mishra, *J. Cryst. Growth* **170**, 340 (1997).
- <sup>6</sup>O.-H. Nam, M. D. Bremser, B. L. Ward, R. J. Nemanich, and R. F. Davis, *Jpn. J. Appl. Phys., Part 2* **36**, L532 (1997).
- <sup>7</sup>O.-H. Nam, M. D. Bremser, B. L. Ward, R. J. Nemanich, and R. F. Davis, in *III-V Nitrides*, edited by F. A. Ponce, T. D. Moustakas, I. Akasaki, and B. A. Monemars [*Mater. Res. Soc. Symp. Proc.* **449**, 107 (1997)].
- <sup>8</sup>*High Voltage Vacuum Insulation*, edited by R. V. Latham (Academic, San Diego, 1995).
- <sup>9</sup>J. D. Shovlin and M. E. Kordesch, *Appl. Phys. Lett.* **65**, 863 (1994).
- <sup>10</sup>M. D. Bremser, W. G. Perry, T. Zheleva, N. V. Edwards, O. H. Nam, N. Parikh, D. E. Aspnes, and R. F. Davis, *The MRS Internet Journal of Nitride Semiconductor Research*, <http://nsr.mij.mrs.org/1/8/> **1** (1996).
- <sup>11</sup>R. Schlessler, M. T. McClure, B. L. McCarron, and Z. Sitar, *J. Appl. Phys.* **82**, 5763 (1997).
- <sup>12</sup>E. Bauer, M. Mundscha, W. Swiech, and W. Telieps, *NATO Advanced Research Workshop on the Evaluation of Advanced Semiconductor Materials by Electron Microscopy* (Plenum, New York, 1989).
- <sup>13</sup>E. Bauer, *Inst. Phys. Conf. Ser.* **119**, 1 (1991).
- <sup>14</sup>H. Bethge and M. Klaua, *Ultramicroscopy* **11**, 207 (1983).
- <sup>15</sup>R. M. Tromp and M. C. Reuter, *Ultramicroscopy* **50**, 171 (1993).
- <sup>16</sup>L. H. Veneklasen, *Rev. Sci. Instrum.* **63**, 5513 (1992).
- <sup>17</sup>L. Wegmann, *J. Microsc.* **96**, 1 (1972).